Catalysis Science & Technology

ROYAL SOCIETY OF CHEMISTRY

PAPER

View Article Online
View Journal

Cite this: DOI: 10.1039/d1cy00376c

Rational engineering of *Acinetobacter tandoii* glutamate dehydrogenase for asymmetric synthesis of L-homoalanine through biocatalytic cascades†

Liuzhu Wang, ‡ Shiqing Diao, ‡ Yangyang Sun, Shuiqin Jiang, Yan Liu, Hualei Wang * and Dongzhi Wei *

Received 2nd March 2021,
Accepted 22nd April 2021

DOI: 10.1039/d1cy00376c

rsc.li/catalysis

L-Homoalanine, a useful building block for the synthesis of several chiral drugs, is generally synthesized through biocascades using natural amino acids as cheap starting reactants. However, the addition of expensive external cofactors and the low efficiency of leucine dehydrogenases towards the intermediate 2-ketobutyric acid are two major challenges in industrial applications. Herein, a dual cofactor-dependent glutamate dehydrogenase from *Acinetobacter tandoii* (*At*GluDH) was identified to help make full use of the intracellular pool of cofactors when using whole-cell catalysis. Through reconstruction of the hydrophobic network between the enzyme and the terminal methyl group of the substrate 2-ketobutyric acid, the strict substrate specificity of *At*GluDH towards α-ketoglutarate was successfully changed, and the activity obtained by the most effective mutant (K76L/T180C) was 17.2 times higher than that of the wild-type protein. A three-enzyme co-expression system was successfully constructed in order to help release the mass transfer restriction. Using 1 M L-threonine, which is close to the solubility limit, we obtained a 99.9% yield of L-homoalanine in only 3.5 h without adding external coenzymes to the cascade, giving 99.9% ee and a 29.2 g L^{-1} h^{-1} space–time yield. Additionally, the activities of the engineered *At*GluDH towards some other hydrophobic amino acids were also improved to 1.1–11.2 fold. Therefore, the engineering design of some dual cofactor-dependent GluDHs could not only eliminate the low catalytic activity of unnatural substrates but also enhance the cofactor utilization efficiency of these enzymes in industrial applications.

Introduction

Optically pure amino acids can be used as active pharmaceutical ingredients.[1,2] In particular, unnatural amino acids, such as L-homoalanine, D-alanine, L-norvaline, D-phenylalanine, D-tryptophan, and L-3,4-dihydroxy-Phe, are more attractive because they can be artificially endowed with diverse functional groups and are useful chiral intermediates in the pharmaceutical industry.[3] Among these compounds, L-homoalanine is an important chiral building block widely used in the synthesis of chiral pharmaceuticals, such as levetiracetam, brivaracetam, and ethambutol.[4,5] In recent studies focused on cancer treatment, bivalent antagonists of inhibitors of apoptosis proteins, which contain two L-homoalanine residues, may further facilitate the growth of demand for L-homoalanine.[6]

Biocatalysis may be the best approach to realize an environmentally friendly process and obtain excellent optical purity of L-homoalanine with high efficiency.[7–9] Among various biocatalysts, transaminases (TAs) and amino acid dehydrogenases (AADHs) are two potential enzymes applied in this field. TA reactions usually have high turnover rates, broad substrate specificity, no requirements for cofactors and neutral equilibrium constants.[10,11] Park *et al.* synthesized L-homoalanine by ω-transaminase using benzylamine as an amino donor and obtained 91% conversion.[12] Silva *et al.* studied the asymmetric conversion of 2-ketobutyric acid to either L- or D-homoalanine by aminotransferase.[13] However, their industrial applications are limited by the equilibrium of the reaction. Amino acid dehydrogenases, which catalyze the reductive amination of α-keto acids by consuming cheap ammonia and the equivalent cofactor NAD(P)H, are the most promising catalysts for effective synthesis of L-homoalanine.[14,15] α-Keto acids have been reported as initial reactants for the production of L-homoalanine in previous

State Key Laboratory of Bioreactor Engineering, New World Institute of Biotechnology, East China University of Science and Technology, Shanghai, 200237, China. E-mail: hlwang@ecust.edu.cn, dzhwei@ecust.edu.cn

† Electronic supplementary information (ESI) available: Supporting figures and tables. See DOI: 10.1039/d1cy00376c

‡ Liuzhu Wang and Shiqing Diao contributed equally to this work.

studies. For example, Galkin *et al.* employed a LeuDH from *Thermoactinomyces intermedius* (*Ti*LeuDH) and achieved a yield of 88% and a concentration of 0.35 M within 12 h (3 g L^{-1} h^{-1} space–time yield), indicating the relatively low activity of *Ti*LeuDH.[16] Additionally, currently reported AADHs generally exhibited low activity towards substrates, such as 2-ketobutyric acid. Moreover, α-keto acids are typically quite expensive, and the use of 2-ketobutyric acid as a starting reactant may be impractical, particularly in industrial applications for which high substrate concentrations are required.

Based on these concepts, an improved approach through cascades for the production of L-homoalanine using cheaper natural amino acids as substrates has been developed. First, prochiral intermediate 2-ketobutyric acid was prepared from inexpensive L-threonine or L-methionine through dehydratases, and this compound was then reductively aminated to L-homoalanine by L-AADHs. For example, Tao *et al.* coupled a threonine dehydratase (TD) with a LeuDH from *Bacillus cereus* (*Bc*LeuDH) in a cascade to reduce the cost of using α-keto acids and improve the efficiency of the reaction.[17] The concentration of the substrate can be as high as 1 M, with a yield of 97.3%. However, this process required a long time (approximately 16 h; 6.37 g L^{-1} h^{-1} space–time yield) because of the mismatch in the activities of TD and *Bc*LeuDH. The first step mediated by TD is generally conducted with high efficiency, even if the substrate concentration is high (up to 1 M), and complete conversion can be obtained within a short time. Indeed, reductive amination is still a rate-limiting step in cascades owing to the low activity of LeuDH. Although many researchers have attempted to improve the activity of LeuDHs towards 2-ketobutyric acid, the results have not been satisfactory. For example, Zhou *et al.* and Xu *et al.* increased the space–time yields to 6.86 and 8.59 g L^{-1} h^{-1}, respectively, through rational or semi-rational engineering.[18,19] And the space–time yield was still low owing to the unsatisfactory catalytic efficiency caused by LeuDHs; thus, this approach could not meet the demands of industrial applications.

In addition to the problem described above, the redox reaction involved in this pathway requires expensive cofactors, such as NAD(P)H, to provide reducing equivalents. Even with an efficient coenzyme regenerating system, a minimum amount of 0.1 mM NAD(P)H is generally required for high catalytic efficiency in AADH-mediated reactions, contributing to the high cost of the reaction. However, in some other redox reactions, external coenzymes are not required when using whole cells or crude enzyme solutions as catalysts, such as those catalyzed by ketoreductases.[20–22] To achieve high performance of biocatalysis without additional NAD(P)H, the turnover efficiency of the cofactors could be improved by modifying the affinity of cofactors with enzymes or screening related enzymes with both NADH and NADPH dependence to make full use of the intracellular pool of cofactors. The former approach has proved to be effective in most instances, while it requires much effort to change the efficiency of coenzyme utilization, and a systematically effective method has not yet been reported.[23–26] As the three most commonly used AADHs, LeuDHs and PheDHs are strictly NADH dependent, whereas some glutamate dehydrogenases (GluDHs) are dependent on dual cofactors and may serve as good candidates for avoiding the requirement for additional cofactors in whole-cell catalysis.

Accordingly, in this study, we aimed to develop a highly efficient approach for reductive amination without the addition of external cofactors using a dual cofactor-dependent GluDH from *Acinetobacter tandoii* (*At*GluDH) to replace LeuDHs that are traditionally used to catalyze α-keto acids with hydrophobic side chains. Our results provided important insights into the use of dual cofactor-dependent GluDHs for industrial applications.

Results and discussion

Characterization of the enzymes in the cascade reaction

A two-step cascade reaction using cheap and easily accessible L-threonine as a starting material was employed for the synthesis of L-homoalanine (Scheme 1). A threonine dehydratase (*Ec*TD) from *Escherichia coli* with reported high activity was used for the dehydration of L-threonine to produce the intermediate 2-ketobutyric acid. In order to catalyze the reductive amination of 2-ketobutyric acid efficiently, we screened dual cofactor-dependent GluDHs with high activity in the library of our laboratory. Among them, the GluDH (*At*GluDH) from *Acinetobacter tandoii* was chosen for further study due to its highest specific activity (Tables S1 and S2†). Also, its melting temperature and half-life of inactivation at 50 °C is 53.7 °C and 20.4 h, respectively, indicating its good thermostability (Fig. S1†). Coupled with a glucose dehydrogenase (*Bm*GDH) from *Bacillus megaterium*, which is also a dual cofactor dependent on the regeneration of cofactors in cells, the reaction could recycle NADH and NADPH simultaneously, thereby improving the efficiency of the coenzymes.

We then evaluated the efficiency of the two steps in the cascade. Notably, the specific activities of *Ec*TD, *At*GluDH, and *Bm*GDH were found to be 734.1 ± 28.7, 57.3 ± 9.1, and 695.7 ± 34.5 U mg^{-1}, respectively. Obviously, the activity of *At*GluDH was much lower than the activities of the other two enzymes, suggesting that this may be the rate-limiting enzyme in the cascade. Before starting a cascade reaction, we first studied the effect of pH on the reaction (Fig. S2†), and it

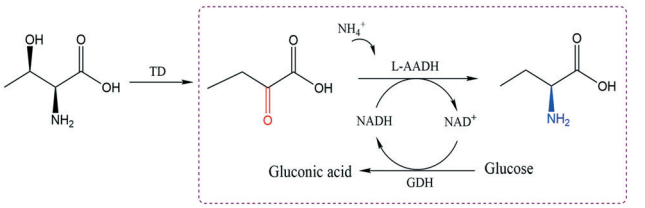

Scheme 1 Cascade reaction catalyzed by threonine dehydratase, L-amino acid dehydrogenase and glucose dehydrogenase.

has been found that pH 9.5 was the optimum pH for the cascade, so 200 mM NH_4Cl/NH_4OH buffer (pH 9.5) was used as the reaction buffer. The effects of the substrate concentrations on the activity of *Ec*TD and *At*GluDH were then studied. For *Ec*TD, at a starting concentration of 1 M L-threonine, the residual amount of the substrate was not detectable after 10 min, demonstrating the high activity of *Ec*TD in the cascade (Fig. S3†). For *At*GluDH, when the substrate concentration reached 600 mM, the conversion was 93% within 24 h (Fig. S4†). This was much lower than the 99% conversion of natural LeuDHs at a concentration of 1 M, as has been reported previously, suggesting that the second step mediated by *At*GluDH was the rate-limiting step. This result was consistent with the strict substrate specificity of GluDHs, which were used as catalysts for reductive amination. Because the side chains of the two substrates (α-ketoglutarate and 2-ketobutyric acid) had different requirements for the polarity of the active pocket, the efficiency of *At*GluDH was low towards 2-ketobutyric acid. In order to match the efficiencies of the two steps, *At*GluDH should be further engineered to change its substrate specificity from the native substrate α-ketoglutarate to α-keto acids with more hydrophobic side chains based on our understanding of the structure.

Construction of an interaction network between *At*GluDH and 2-ketobutyric acid

To elucidate the interaction of *At*GluDH with its native substrate or 2-ketobutyric acid, a homology model of *At*GluDH was first constructed based on the crystal structure of GluDH from *Burkholderia thailandensis* (PDB ID: 4XGI, resolution: 2.0 Å) in complex with its NAD^+ cofactor and native substrate α-ketoglutarate with the highest sequence identity (62%) between the enzymes. The substrate 2-ketobutyric acid was then docked into *At*GluDH using AutoDock (Fig. S5†).[27]

AADHs have two primary conformations, *i.e.*, the substrate binding "open" state and the catalytic "closed" state in the aqueous phase. To study the interactions between the substrate and the enzyme, we evaluated the structural alignment between *At*GluDH and GluDH from *Clostridium symbiosum* (PDB ID: 1AUP and 1BGV) and GluDH from *Corynebacterium glutamicum* (PDB ID: 5IJZ), which showed a catalytic closed conformation.[28–31] Residues K76, S355, R192, and T180 were conserved and played important roles in substrate binding in these GluDHs (Fig. S6†). The positively charged K76 and R192 stabilized the negatively charged α-ketoglutarate through charge–charge interactions and cooperated with residue S355 to modulate the substrate specificity of GluDHs (Fig. 1A). At the same time, these three residues together with T180 provided a hydrophilic environment to accommodate the γ-carboxyl of α-ketoglutarate in the active pocket.[32] Compared with α-ketoglutarate, 2-ketobutyric acid has one less carboxyl group at the γ-position and harbors a more hydrophobic side chain. Therefore, the original hydrophilic active pocket was not suitable for the stable binding of 2-ketobutyric acid, leading to

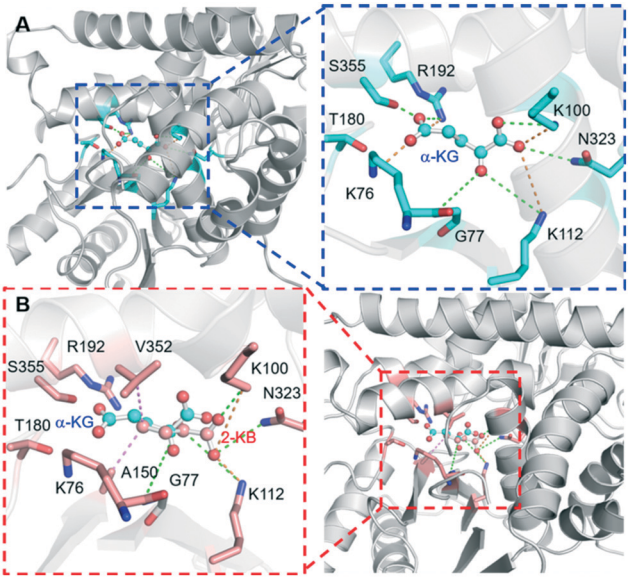

Fig. 1 (A) Illustration of the native substrate α-ketoglutarate binding position in the active site of *At*GluDH. Orange-colored and green-colored dotted lines represent hydrogen bonds with an electrostatic character and hydrogen bonds without an electrostatic character, respectively, contributing to the binding of the α-ketoglutarate. (B) The difference in the binding position between the native substrate α-ketoglutarate and the docking substrate 2-ketobutyric acid (2-KB) in *At*GluDH. Residues having interactions with the 2-ketobutyric acid directly or indirectly are shown as sticks. Purple-colored and green-colored dotted lines represent hydrophobic interactions and hydrogen bonds, respectively, contributing to the binding of the 2-ketobutyric acid.

an obvious deviation at the active site and resulting in decreased catalytic activity (57.3 U mg^{-1} for 2-ketobutyric acid, 2185.8 U mg^{-1} for α-ketoglutarate) (Fig. 1B). The analysis of the affinity between *At*GluDH-WT and the natural substrate α-ketoglutarate or 2-ketobutyrate showed that *At*GluDH has a very strong affinity for α-ketoglutarate (for 2-ketobutyric acid, K_m = 4.12 mM, k_{cat} = 0.53 s^{-1}; for α-ketoglutarate, K_m = 0.07 mM, k_{cat} = 16.71 s^{-1}), indicating that the strict substrate specificity of wild-type glutamate dehydrogenases limited their catalytic activity on other unnatural substrates.

To obtain high activity towards 2-ketobutyric acid, a more hydrophobic environment is crucial, and the interaction network between 2-ketobutyric acid and the enzyme should be rebuilt. Among the four conserved polar residues in the active pocket of *At*GluDH, R192, which has a hydrogen bond with the carbonyl group of the nicotinamide of NADH, was not selected for further engineering. The other three residues were then mutated to alanine and valine in order to quickly analyze the effects of different steric hindrances, polarities and straight or branched chains on the activities. Finally, six mutants, *i.e.*, K76A/V, S355A/V, and T180A/V, were generated.

Analysis of mutant activities

The reductive amination activities of the mutants and wild-type *At*GluDH toward 2-ketobutyric acid were determined

(Fig. S7†). Among the selected six mutants, only mutations at K76 showed beneficial activities, and the activity of K76V showed the highest improvement (up to 7.4-fold) compared with that of the wild-type protein. These results may be attributed to the observation that hydrophobic residues with longer side chains (like valine compared with alanine) can form more efficient interactions with 2-ketobutyric acid, which has one less carboxyl group on the substrate compared with α-ketoglutarate. Based on these speculations, residue K76 was mutated to other hydrophobic amino acids with different side chain dimensions (G, A, V, L, and I) to study the effects of different side chain lengths on the substrate. All mutants showed consistent results, as expected. Notably, K76L (960.6 U mg^{-1}) showed the highest efficiency (increase of 16.8-fold) compared with the wild-type protein. The longest side chain (from the leucine residue) at site 76 was likely to accommodate the structurally small size of 2-ketobutyric acid, resulting in beneficial interactions.

The mutation of S355 and T180 to more hydrophobic amino acids did not yield the expected results. The S355A mutant maintained 80% of the activity of the wild-type protein, whereas the S355V mutant lost all its activity.[28] This may be because the mutations disrupted the interactions between residues S355 and R192/V352, the latter two of which directly or indirectly interacted with the substrate to stabilize the conformations. Accordingly, no further modifications were made to this site. Both T180A and T180V showed decreased catalytic activity, *i.e.*, 67.2% and 61.0% of the activity of the wild-type protein, respectively. These results could be explained by the observation that mutating T180, which is located in the hinge region close to the solvent, to a hydrophobic amino acid may cause loss of the inherent stability of the hydration structure. Therefore, we mutated T180 to other polar residues with small side chains (Ser and Cys) in order to avoid steric hindrance at the bulky pyrrolidine ring of P151. The mutants T180S and T180C showed 11.5- and 14.4-fold enhanced activities, respectively, suggesting that mutation of T180 was involved in the reconstruction of the interaction network and facilitated biocatalysis. To explore the potential synergistic effect, a double mutant K76L/T180C was constructed; the mutant showed the highest activity (985.7 U mg^{-1}), which was 17.2 times higher than that of the wild-type enzyme. However, it was 1.03-fold and 1.19-fold higher than the mutants K76L and T180C, respectively, and there was no obvious synergy between these two mutations.

To elucidate the molecular mechanisms of these beneficial mutations, 2-ketobutyric acid was docked into the active site of the *At*GluDH-WT (Fig. 2A) and mutants (Fig. 2B–D) through computational simulation. The mutant K76L provided a more hydrophobic environment at the active site and generated interactions with the γ-methyl group of 2-ketobutyric acid directly (Fig. 2B). Moreover, K76L also formed hydrophobic interactions with A150 and V352, which were the only two residues that interacted with the side chain of the substrate. These interaction forces formed a hydrophobic network to stabilize the substrate in the catalytic closed conformation. For mutant T180C, substitution of the threonine residue with a less polar cysteine reduced the hydrophilicity of the bottom of the active pocket and altered the hydrophobic microenvironment of the substrate binding pocket (Fig. 2C). At the same time, mutant T180C contributed to the stable conformation of the substrate in the active pocket by indirect interactions with the substrate through generating hydrophobic forces with residues A150 and S355.

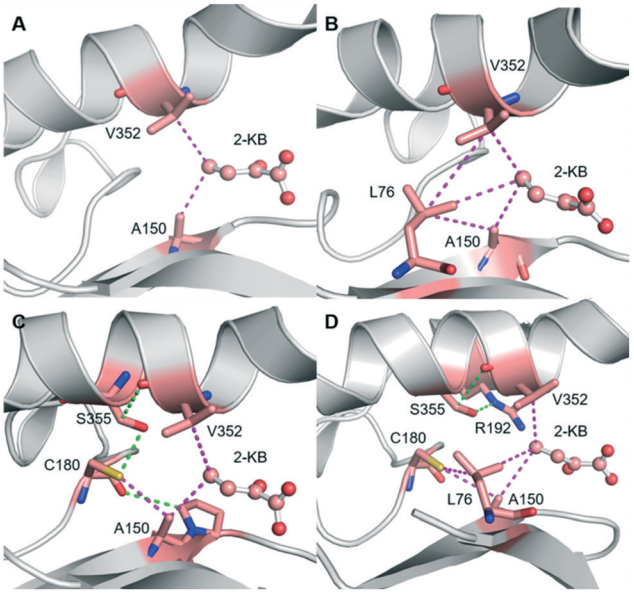

Fig. 2 (A) Docking of 2-ketobutyric acid into *At*GluDH-WT. (B) Docking of 2-ketobutyric acid into *At*GluDH-K76L. (C) Docking of 2-ketobutyric acid into *At*GluDH-T180C. (D) Docking of 2-ketobutyric acid into *At*GluDH-K76L/T180C. Residues having interactions with the 2-ketobutyric acid directly or indirectly are shown as sticks. Purple-colored and green-colored dotted lines represent hydrophobic interactions and hydrogen bonds, respectively, contributing to the binding of the 2-ketobutyric acid.

The binding free energy of 2-ketobutyric acid was estimated through the molecular mechanics Poisson–Boltzmann (generalized Born) surface area method, which could explain the enhancement of activity by the double mutant K76L/T180C. For the wild-type *At*GluDH, the binding free energy was calculated to be −57.56 ± 10.16 kcal mol^{-1}; this value was decreased to −62.44 ± 6.81 kcal mol^{-1} in *At*GluDH–K76L/T180C (Table S4†). These findings demonstrated that the mutant K76L/T180C showed thermodynamically stronger binding forces with the substrate compared with the wild-type protein, consistent with the experimentally higher catalytic activity. Moreover, the distance (d_c) between the reactive carbonyl carbon (C2) of the substrate and the hydride donating/accepting carbon (C4) of the nicotinamide of the coenzyme was measured in molecular dynamics simulations as a crucial catalytic distance, as reported for AADHs (Fig. S8†).[33–35] The data showed that the d_c^{avg} of K76L/T180C was 0.6 Å shorter than that of the wild-type protein. The reduction of the catalytic

crucial distance was conducive to increasing the reaction efficiency, increasing the catalytic activity of mutant K76L/T180C towards 2-ketobutyric acid.

Kinetic parameters and substrate specificity analysis

To explicate the reason for the improved activity in biocatalysis, the kinetic parameters of purified enzymes towards 2-ketobutyric acid were determined (Table 1). The K_m values of K76L, T180C, and K76L/T180C were all lower than that of the wild-type protein, indicating that the enzyme had increased affinity with the substrate. Moreover, the K_m value of the double mutant K76L/T180C was 2.52 ± 0.21 mM, which was lower than that of the wild-type protein (4.12 ± 0.82 mM), demonstrating its high affinity than that of the wild-type protein for 2-ketobutyric acid. The catalytic efficiencies (k_{cat}/K_m) of the mutants K76L, T180C, and K76L/T180C were 7.9-, 7.5-, and 9.9-fold higher than that of the wild-type protein, respectively, demonstrating enhanced activity toward 2-ketobutyric acid.

Next, to elucidate the substrate spectrum of the engineered enzyme, *At*GluDH and its mutants were characterized using various α-keto acids with different structures (Table 2). Compared with the wild-type *At*GluDH enzyme, the mutants K76L, T180C, and K76L/T180C showed decreased activity when employing α-ketoglutarate, the native substrate of GluDHs. All mutants showed a strong preference for unbranched aliphatic nonpolar α-keto acids, particularly 2-oxopentanoic acid, which is similar in structure to 2-ketobutyric acid but contains one more carbon atom in the skeleton. In our analysis of branched aliphatic substrates, the mutants K76L and K76L/T180C showed higher activity towards short-branched α-keto acids, such as S5 (2.3- or 2.5-fold) and S8 (2.8- or 3.3-fold), than the wild-type protein. This result may be explained by the efficient anchoring of short-branched α-keto acids in the tailored active pocket by K76L with a bulky leucine.

For aromatic α-keto acids, both the wild-type protein and mutants exhibited low activity owing to significant differences between the structures of aromatic amino acids and the natural substrate of GluDHs. Thus, by reconstructing a new hydrophobic interaction network, the substrate specificity of *At*GluDH was successfully switched from hydrophilic to hydrophobic amino acids.

Table 1 Kinetic parameters of *At*GluDH and its mutants towards 2-ketobutyric acid

Enzyme	k_{cat} (s^{-1})	K_m (mM)	k_{cat}/K_m (mM^{-1} s^{-1})
WT	0.53 ± 0.08	4.12 ± 0.82	0.13
K76L	3.03 ± 0.11	2.96 ± 0.97	1.02
T180C	2.81 ± 0.28	2.88 ± 0.83	0.98
K76L/T180C	3.24 ± 0.13	2.52 ± 0.21	1.29

Reaction conditions: 200 mM NH_4Cl/NH_4OH buffer (pH 9.5), 0.1 mM NADH, 2-ketobutyric acid (0.1–50 mM), and at 30 °C.

Application of *At*GluDH mutants for the synthesis of L-homoalanine by cascades

To verify the application of the mutants (K76L, T180C, and K76L/T180C) in the cascade, a 20 mL reaction was carried out using 1 M L-threonine as a substrate owing to its solubility limit and a low concentration of NADH (0.1 mM) in an aqueous system. Three enzymes, including 3 g L^{-1} *Ec*TD (31.8 U $mg^{-1}_{\text{-DCW}}$), 10 g L^{-1} *At*GluDH (9.2 U $mg^{-1}_{\text{-DCW}}$), and 3 g L^{-1} *Bm*GDH (36.9 U $mg^{-1}_{\text{-DCW}}$), were added as lyophilized cells. Compared with the wild-type protein, all three mutants showed higher catalytic efficiency (Fig. 3). The double mutant K76L/T180C exhibited the highest efficiency, providing a yield of 99.9% within 2 h. The mutants K76L and T180C showed a 99.9% yield within 2.5 and 3 h, respectively. The space–time yields of the three mutants varied from 34.4 to 51.1 g L^{-1} h^{-1}, which are the highest level reported in current studies. However, a high enzyme loading (16 g L^{-1}) was applied when feeding the three enzymes separately in the cascade. Thus, mass transfer in different cells may be challenging, and downstream separation and purification may be more complex.

To further improve the efficiency of the reaction, *Ec*TD, *At*GluDH, and *Bm*GDH were expressed simultaneously in a single cell. Using lyophilized cells with the same activity as *At*GluDH, as described above, the co-expression system reached a yield of 99.9% L-homoalanine within 100 min (Fig. 3). The co-expression of the three enzymes greatly decreased fermentation costs and improved catalytic efficiencies, suggesting applications in industrial manufacturing. To investigate the ability of the dual cofactor-dependent *At*GluDH to utilize intracellular cofactors by whole-cell catalysis, a three-enzyme co-expression strain was used without the addition of NAD(P)H. The results showed that a yield of 99.9% L-homoalanine was achieved after 3.5 h without the addition of NAD(P)H, and an isolated yield of 78.2% was obtained. Thus, the economic cost of industrial production was significantly reduced, and the route of reductive amination for production of L-homoalanine became more competitive.

Experimental

Materials

The chemicals used in the experiment including 2-ketobutyric acid, L-threonine, L-2-aminobutyric acid, NH_4Cl, and $NH_3{\cdot}H_2O$ were purchased from Aladdin Reagents (Shanghai, China). The restriction enzymes *Xho*I, *Bam*HI and *Nde*I were obtained from TaKaRa (Shanghai, China). The enzymes used for the experiment including PrimeSTAR, KOD-One and T4 DNA ligase were also purchased from TaKaRa (Shanghai, China).

Gene cloning and site-directed mutagenesis

The genomic DNAs from *Acinetobacter tandoii*, *Escherichia coli* and *Bacillus megaterium* were extracted using a Bacteria DNA Kit from Tiangen (Shanghai, China). We designed

Table 2 Specific activity of wild type *At*GluDH and mutants K76L and T180C and K76L/T180C towards various α-keto acids

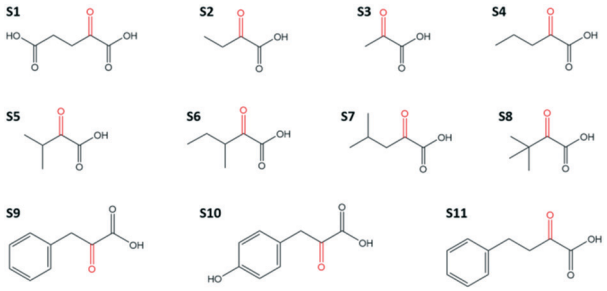

	Specific activity[a] (U mg^{-1})			
S	Wild type	K76L	T180C	K76L/T180C
1	2185.8 ± 151.7	947.7 ± 88.5	1271.5 ± 132.5	864.5 ± 79.8
2	57.3 ± 9.1	960.6 ± 23.5	827.5 ± 21.7	985.7 ± 18.1
3	159.6 ± 13.2	196.5 ± 9.9	114.6 ± 11.3	115.8 ± 5.7
4	44.1 ± 2.4	495.2 ± 32.6	212.8 ± 13.3	327.4 ± 14.5
5	34.6 ± 28.5	77.9 ± 11.5	32.7 ± 8.4	88.0 ± 44.9
6	43.2 ± 17.7	38.7 ± 13.2	50.4 ± 29.6	25.1 ± 12.7
7	19.3 ± 12.4	14.6 ± 7.3	21.4 ± 13.6	17.9 ± 11.2
8	9.1 ± 5.3	25.5 ± 8.4	5.3 ± 3.3	29.7 ± 17.6
9	12.7 ± 0.9	15.6 ± 1.8	11.1 ± 2.5	12.2 ± 1.2
10	2.5 ± 0.3	3.3 ± 0.2	2.9 ± 0.5	3.2 ± 0.3
11	4.1 ± 0.3	3.2 ± 0.8	2.5 ± 0.1	4.9 ± 0.2

[a] Specific activity was determined with purified proteins. Reaction conditions: 200 mM NH_4Cl/NH_4OH buffer (pH 9.5), 0.1 mM NADH, appropriate substrate concentrations and at 30 °C.

oligonucleotide primers with restriction sites based on the gene sequence found in the NCBI. The amplified DNA fragments were double-digested with the corresponding restriction endonuclease and inserted into the expression vector of pET-28a plasmid (Novagen, Shanghai, China). The plasmids constructed were transformed into *E. coli* BL21 (DE3) cells. Site-directed mutagenesis of *At*GluDH was conducted using a KOD-One site mutation kit from Toyobo Co., Ltd. (Japan). The primer comprising required codons for mutations was designed and listed in Table S3.† After amplification, *Dpn*I was added to specifically remove the methylated template DNA chain, and then T4 polynucleotide kinase and Ligation high in the kit were used to enable the digested products to self-cyclize. After transformation, a single colony was picked and inoculated into Luria-Bertani (LB) broth containing kanamycin (50 μg mL^{-1}), and the DNA sequencing for the mutations was conducted by Tsingke (Shanghai, China) after growing for 12 h.

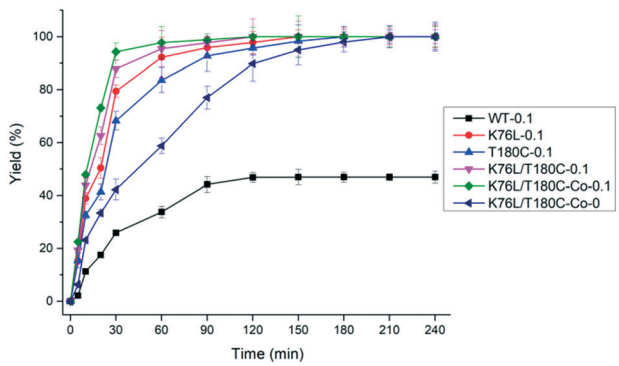

Fig. 3 Cascade reaction curves of *At*GluDH and mutants using 1 M L-threonine as a substrate. Enzyme loading of WT-0.1, K76L-0.1, T180C-0.1 and K76L/T180C-0.1: 3 g L^{-1} *Ec*TD, 10 g L^{-1} *At*GluDH and 3 g L^{-1} *Bm*GDH using lyophilized cells. Enzyme loading of the co-expression system (K76L/T180C-Co-0.1 and K76L/T180C-Co-0): 12 g L^{-1} lyophilized cells. The amount of NADH added into the reaction was 0.1 mM (WT-0.1, K76L-0.1, T180C-0.1, K76L/T180C-0.1 and K76L/T180C-Co-0.1) and 0 mM (K76L/T180C-Co-0). Error bars represent the standard deviation of three independent experiments.

Expression and purification of proteins

The recombinant cells were cultured on an agar plate for 12 hours at 37 °C, and then single colonies were picked into tubes containing 5 ml of LB medium and 50 μg ml^{-1} kanamycin. After that, the cells were cultured at 37 °C with 200 rpm for 10–12 hours. Then, they were transferred into flasks containing 200 ml of LB medium and 50 μg ml^{-1} kanamycin, and cultured at 37 °C with 200 rpm for about 3.5 hours. When the optical density value (λ = 600 nm, OD600) reached 0.6 to 0.8, 0.1 mM IPTG was added for induction, and the cells were incubated for 18 hours at 20 °C with 200 rpm. These recombinant cells were then centrifuged at 8000 rpm for 10 minutes at 4 °C, washed with 0.5% NaCl solution three times and lyophilized using a vacuum freeze dryer or resuspended in 20 mM PB buffer (pH 8.0) on ice. If resuspended, the recombinant cells were disrupted by

ultrasonication and centrifuged at 8000 rpm for 30 minutes at 4 °C to remove the unbroken cells and cell debris. The supernatant was loaded onto a Ni-NTA column, and the 6× His-tagged protein bound to the Ni-NTA column at a flow rate of 1 ml min^{-1}, and then was eluted with 20 mM, 50 mM, 100 mM, 250 mM, and 500 mM imidazole eluents at the same flow rate. The protein purity of the collected fractions was examined by sodium dodecyl sulfate polyacrylamide gel electrophoresis (SDS-PAGE). The fractions containing the target proteins were gathered and dialyzed against 20 mM PB buffer (pH 8.0) for desalting. The enzyme solution was concentrated, mixed with 20% (v/v) glycerol and stored at −80 °C for further use.

Enzyme assay

A 1 mL scale reaction mixture containing a certain amount of purified *Ec*TD, L-threonine (200 mM) and 200 mM NH_4Cl–NH_4OH (200 mM, pH 9.5) was incubated at 30 °C, and then quenched with 5 M KOH (100 μL) at default time intervals. The samples were analyzed by HPLC.

The activities of GluDHs were measured at 30 °C. They were measured indirectly by monitoring the absorbance at 340 nm (ε = 6220 M^{-1} cm^{-1}) to obtain the concentration of consumed NADH during the reductive amination reaction. The reaction mixture consisted of 2-ketobutyric acid (50 mM), NADH (0.1 mM), and NH_4Cl–NH_4OH (200 mM, pH 9.5) buffer, and a certain amount of crude enzyme extract or purified enzyme solution was added to start the reaction.

For *Bm*GDH, the reaction mixture contained a certain amount of purified *Bm*GDH, glucose (200 mM), NAD^+ (0.1 mM) and 200 mM NH_4Cl–NH_4OH (200 mM, pH 9.5). The activity of *Bm*GDH was measured at 30 °C by using a similar method to that of *At*GluDH.

One unit of enzyme activity is defined as the amount of enzyme required to catalyze the conversion of 1 μmol substrate per minute. The method of Bradford was used to measure the concentrations of the protein.

Preparative application of *At*GluDHs for the synthesis of L-homoalanine

The reaction system for producing L-homoalanine from L-threonine through a cascade contained 1 M L-threonine, 1.2 M glucose, NADH (0.1 mM or 0 mM), *Ec*TD (3 g L^{-1}), *At*GluDH (WT or mutants) (10 g L^{-1}) and *Bm*GDH (3 g L^{-1}) which were prepared as lyophilized cells or a certain amount of co-expressed cells and 200 mM NH_4Cl/NH_4OH buffer (pH 9.5). The final volume of the reaction mixture was 20 mL. The reaction was conducted at 30 °C, and the pH was automatically adjusted to 9.5 by titrating with $NH_3{\cdot}H_2O$. Aliquots (100 μL) of the reaction mixture were taken at different time intervals and quenched with 100 μL KOH (5 M), and then analyzed by HPLC. The product was separated and purified using the method described by Yin *et al.*[36] and analyzed by NMR (Fig. S11†).

Kinetic analysis

The kinetic parameters were measured at 30 °C and pH 9.5. Using purified GluDH and its variants, the enzyme activities at different substrate concentrations (0.1–50 mM 2-ketobutyric acid or 0.01–10 mM α-ketoglutarate) were measured at a fixed NADH concentration (0.1 mM). Importing the obtained data, the relationship curve between the initial reaction rate (v_i) and the substrate concentrations was drawn, and the Michealis–Menten equation fitting was used to get the v_{max} and K_m values. The k_{cat} values were calculated from v_{max} and the concentration of the enzymes.

Co-expression of the enzymes

The open reading frame (ORF) of GluDH from pET28a-GluDH was cloned into the backbone of pET28a-GDH in front of GDH to create pET28a-GluDH-GDH. The pACYC184 vector had been split by *Hind*III to obtain a linker vector backbone, and then the ORF of TD from pET28a-TD was inserted to create pACYC184-TD. Then pET28a-GluDH-GDH and pACYC184-TD were co-transformed into *E. coli* BL21(DE3) to have a three protein co-expression.

Analytical methods

Analysis of L-homoalanine and L-threonine: HPLC detection conditions: column Agilent C18 (5 μm × 4.6 mm × 250 mm), mobile phase: *V* (acetonitrile) : *V* (0.02 mol L^{-1} Na_2HPO_4 buffer (pH 7.2)) = 15 : 85, UV detection wavelength: 360 nm, column temperature: 30 °C, flow rate: 1.0 mL min^{-1}. Sample derivatization conditions: 100 μL of the testing sample diluted by a certain multiple was taken and mixed with 100 μL of 0.5 mol L^{-1} $NaHCO_3$ solution and 50 μL of 1% 2,4-dinitrofluorobenzonitrile (DNFB) solution. The samples were incubated at 60 °C in the dark for 1 h, cooled to room temperature after the reaction, and finally mixed with 750 μL NaH_2PO_4/Na_2HPO_4 buffer (0.2 mol L^{-1}, pH 7.0).

Analysis of 2-ketobutyric acid: COSMOSIL packed column PBr (4.6 ID × 250 mm), mobile phase: pure water containing 0.1% H_3PO_4, UV detection wavelength: 210 nm, column temperature: 30 °C, flow rate: 0.8 mL min^{-1}.

Chiral analysis of L-homoalanine: column SCAS SUMICHIRAL OA-5000 L (5 μm × 4.6 mm × 150 mm), mobile phase: a liter of water containing 3 mL acetonitrile and 0.5 g $CuSO_4$, UV detection wavelength: 254 nm, column temperature: 35 °C, flow rate: 0.8 mL min^{-1}.

Conclusions

In summary, to efficiently and economically synthesize L-homoalanine, a novel *At*GluDH with dual cofactor dependency was identified. By reconstructing an interaction network between the enzyme and the substrate, the strict substrate specificity of *At*GluDH was altered, and a high catalytic efficiency towards 2-ketobutyric acid was obtained. Coupled with an efficient *Ec*TD, the adverse effects on the catalytic efficiency caused by the rate-limiting step in the

cascade were successfully alleviated, and a high substrate loading of up to 1 M and a high space–time yield of 29.2 g L^{-1} h^{-1} were achieved. When combined with the dual cofactor-dependent *Bm*GDH, the cascade reaction could be efficiently carried out without the addition of external cofactors, suggesting great advantages in industrial production. Furthermore, increased activities toward some hydrophobic amino acids were obtained, indicating that the substrate spectrum of *At*GluDH was expanded.

Conflicts of interest

There are no conflicts to declare.

Acknowledgements

This work was supported by the National Natural Science Foundation of China (No. 21776084).

Notes and references

1 J. Fortunak, *Trop. J. Pharm. Res.*, 2008, **7**, 865–867.
2 M. Hoehne and U. T. Bornscheuer, *ChemCatChem*, 2010, **1**, 42–51.
3 M. A. Blaskovich, *J. Med. Chem.*, 2016, **59**, 10807.
4 M. A. Martínez-Granero, A. García-Pérez and F. Montañes, *Neuropsychiatr. Dis. Treat.*, 2010, **6**, 309–316.
5 E. Falk, C. Laura and P. Marisa, *Br. J. Clin. Pharmacol.*, 2014, **77**, 612–617.
6 H. L. Perez, C. Chaudhry, S. L. Emanuel, C. Fanslau and R. M. Borzilleri, *J. Med. Chem.*, 2015, **58**, 1556–1562.
7 R. N. Patel, *ACS Catal.*, 2011, **1**, 1056–1074.
8 D. M. Solano, P. Hoyos, M. J. Hernáiz, A. R. Alcántara and J. M. Sánchez-Montero, *Bioresour. Technol.*, 2012, **115**, 196–207.
9 A. S. Bommarius, *Annu. Rev. Chem. Biomol. Eng.*, 2015, **6**, 319–345.
10 E. Heuson, F. Charmantray, J. L. Petit, V. D. Berardinis and T. Gefflaut, *Adv. Synth. Catal.*, 2019, **361**, 778–785.
11 P. Eul-Soo, D. Joo-Young and S. Jong-Shik, *Org. Biomol. Chem.*, 2013, **11**, 6929–6933.
12 E. Park, M. Kim and J. S. Shin, *Adv. Synth. Catal.*, 2010, **352**, 3391–3398.
13 M. Silva, I. Costa, R. De Souza and U. Bornscheuer, *ChemCatChem*, 2019, **11**, 407–411.
14 N. Krall, C. F. Da, O. Boutureira and G. J. Bernardes, *Nat. Chem.*, 2016, **8**, 103.
15 M. Sharma, J. Mangas-Sanchez, N. J. Turner and G. Grogan, *Adv. Synth. Catal.*, 2017, **359**, 2011–2025.
16 A. Galkin, L. Kulakova, T. Yoshimura, K. Soda and N. Esaki, *Appl. Environ. Microbiol.*, 1997, **63**, 4651–4656.
17 R. Tao, J. Yu, F. Zhu and Y. Sheng, *Biotechnol. Lett.*, 2014, **36**, 835–841.
18 J. M. Xu, F. Cheng, F. T. Fu, H. F. Hu and Y. G. Zheng, *Appl. Biochem. Biotechnol.*, 2016, **182**, 898–909.
19 J. P. Zhou, Y. L. Wang, J. J. Chen, M. J. Xu and T. W. Yang, *Biotechnol. J.*, 2018, **14**, 1800253.
20 H. M. Ma, L. L. Yang, Y. Ni, J. Zhang and C. X. Li, *Adv. Synth. Catal.*, 2012, **354**, 1765–1772.
21 L. Huang, H. M. Ma, H. L. Yu and J. H. Xu, *Adv. Synth. Catal.*, 2014, **356**, 1943–1948.
22 Z. Y. Yang, H. W. Fu, W. J. Ye, Y. Y. Xie, Q. H. Liu, H. L. Wang and D. Z. Wei, *Catal. Sci. Technol.*, 2020, **10**, 70–78.
23 N. H. Schlieben, K. Niefind, J. Muller, B. Riebel, W. Hummel and D. Schomburg, *J. Mol. Biol.*, 2005, **349**, 801–813.
24 D. Cui, L. Zhang, Z. Yao, X. Liu, J. Lin, Y. A. Yuan and D. Wei, *Biotechnol. J.*, 2013, **167**, 386–392.
25 Z. N. You, Q. Chen, S. C. Shi, M. M. Zheng, J. Pan, X. L. Qian, C. X. Li and J. H. Xu, *ACS Catal.*, 2018, **9**, 466–473.
26 S. C. Shi, Z. N. You, K. Zhou, Q. Chen, J. Pan, X. L. Qian, J. H. Xu and C. X. Li, *Adv. Synth. Catal.*, 2019, **361**, 4661–4668.
27 G. M. Morris, R. Huey, W. Lindstrom, M. F. Sanner, R. K. Belew, D. S. Goodsell and A. J. Olson, *J. Comput. Chem.*, 2009, **30**, 2785–2791.
28 P. J. Baker, M. L. Waugh, X. G. Wang, T. J. Stillman, A. P. Turnbull, P. C. Engel and D. W. Rice, *Biochemistry*, 1997, **36**, 16109–16115.
29 M. I. H. Khan, H. Kim, H. Ashida, T. Ishikawa, H. Shibata and Y. Sawa, *Biosci., Biotechnol., Biochem.*, 2005, **69**, 1802–1805.
30 L. L. Chen, J. L. Wang, Y. Hu and B. J. Qian, *J. Mol. Model.*, 2013, **19**, 1919–1927.
31 H. F. Son, I. K. Kim and K. J. Kim, *Biochem. Biophys. Res. Commun.*, 2015, **459**, 387–392.
32 T. J. Stillman, P. J. Baker, K. L. Britton and D. W. Rice, *J. Mol. Biol.*, 1993, **234**, 1131–1139.
33 J. L. Vanhooke, J. B. Thoden, N. M. Brunhuber, J. S. Blanchard and H. M. Holden, *Biochemistry*, 1999, **38**, 2326–2339.
34 N. M. Brunhuber, J. B. Thoden, J. S. Blanchard and J. L. Vanhooke, *Biochemistry*, 2000, **39**, 9174–9187.
35 P. Prakash, N. S. Punekar and P. Bhaumik, *J. Biol. Chem.*, 2018, **293**, 6241–6258.
36 X. Yin, Y. Liu, L. Meng, H. Zhou, J. Wu and L. Yang, *Adv. Synth. Catal.*, 2019, **361**, 803–812.

